

# Epithelial Na<sup>+</sup> Channels Are Fully Activated by Furin- and Proastatin-dependent Release of an Inhibitory Peptide from the $\gamma$ -Subunit\*

Received for publication, November 16, 2006, and in revised form, December 19, 2006. Published, JBC Papers in Press, January 1, 2007, DOI 10.1074/jbc.M610636200

James B. Bruns<sup>†1</sup>, Marcelo D. Carattino<sup>†1</sup>, Shaohu Sheng<sup>‡</sup>, Ahmad B. Maarouf<sup>‡</sup>, Ora A. Weisz<sup>‡§</sup>, Joseph M. Pilewski<sup>§¶</sup>, Rebecca P. Hughey<sup>‡§2</sup>, and Thomas R. Kleyman<sup>‡§</sup>

From the <sup>†</sup>Renal-Electrolyte Division and <sup>¶</sup>Division of Pulmonary and Critical Care Medicine, Department of Medicine, and <sup>§</sup>Department of Cell Biology and Physiology, University of Pittsburgh, Pittsburgh, Pennsylvania 15261

Epithelial sodium channels (ENaC) are expressed in the apical membrane of high resistance Na<sup>+</sup> transporting epithelia and have a key role in regulating extracellular fluid volume and the volume of airway surface liquids. Maturation and activation of ENaC subunits involves furin-dependent cleavage of the ectodomain at two sites in the  $\alpha$  subunit and at a single site within the  $\gamma$  subunit. We now report that the serine protease proastatin further activates ENaC by inducing cleavage of the  $\gamma$  subunit at a site distal to the furin cleavage site. Dual cleavage of the  $\gamma$  subunit is predicted to release a 43-amino acid peptide. Channels with a  $\gamma$  subunit lacking this 43-residue tract have increased activity due to a high open probability. A synthetic peptide corresponding to the fragment cleaved from the  $\gamma$  subunit is a reversible inhibitor of endogenous ENaCs in mouse cortical-collecting duct cells and in primary cultures of human airway epithelial cells. Our results suggest that multiple proteases cleave ENaC  $\gamma$  subunits to fully activate the channel.

Epithelial sodium channels (ENaC)<sup>3</sup> are expressed at the apical plasma membrane of cells lining the distal nephron, airway and alveoli, and distal colon, where they play a key role in the regulation of extracellular fluid volume, blood pressure, and airway surface liquid volume. These channels are composed of three homologous subunits, termed  $\alpha$ ,  $\beta$ , and  $\gamma$ . Each subunit has cytosolic amino and carboxyl termini and two membrane-spanning domains separated by a large ectodomain (1–3). The second membrane-spanning domain and the preceding region of each subunit are predicted to form the channel pore (4–7). Proteolysis of ENaC subunit extracellular domains at specific sites has a key role in modulating channel gating (8–10). Mat-

uration of ENaC subunits in *Xenopus* oocytes, Madin-Darby canine kidney (MDCK) cells, and Chinese hamster ovary cells involves furin-dependent cleavage at two sites in the extracellular loop of the  $\alpha$  subunit and at a single site within the extracellular loop of the  $\gamma$  subunit (8). Channels that lack proteolytic processing exhibit markedly reduced activity and enhanced inhibition by external Na<sup>+</sup>, a process referred to as Na<sup>+</sup> self-inhibition (9). ENaC subunit cleavage by furin or exogenous trypsin relieves channels from inhibition by external Na<sup>+</sup> (9, 11). We previously proposed that furin-dependent proteolysis of the  $\alpha$  subunit activates ENaC by disassociating an inhibitory domain ( $\alpha$ Asp-206–Arg-231) from its effector site within the channel complex (10).

Endogenous proteases other than furin likely have a role in the processing and activation of ENaC. A number of serine proteases, referred to as “channel activating proteases,” have been identified that increase ENaC activity when co-expressed with ENaC in heterologous expression systems (12–14). Furthermore, selective serine protease inhibitors that do not block furin, such as aprotinin and bikunin, reduce ENaC activity (14–20). Proastatin is an aprotinin-sensitive “channel activating (serine) protease” that increases ENaC activity when co-expressed in *Xenopus* oocytes (13–15, 20, 21). Proastatin is also thought to have an important role in activating ENaC in collecting duct and airway epithelial cells (16–19, 22, 23).

Because proastatin has been shown to activate ENaC, and we have recently shown that cleavage of the  $\alpha$  and  $\gamma$  subunits is necessary for “normal” channel gating, we examined whether proastatin cleaves ENaC subunits. We observed that proastatin activates ENaC by inducing cleavage of the  $\gamma$  subunit at a site distal to the previously identified furin cleavage site, resulting in an increased channel open probability. Channels with  $\gamma$  subunits that lack the 43-residue tract between the furin and proastatin cleavage sites also have a high open probability. A 43-mer peptide is putatively released from the  $\gamma$  subunit by furin- and proastatin-dependent cleavage, and a synthetic peptide ( $\gamma$ -43) representing this track is an inhibitor of Na<sup>+</sup> channel activity in cortical collecting duct (CCD) and airway epithelia that express endogenous ENaCs.

## EXPERIMENTAL PROCEDURES

**Vectors and Cell Culture**—Wild type, carboxyl-terminal, and double epitope-tagged mouse ENaC subunit cDNAs were previously described (24, 25). The  $\gamma$  subunit mutations were gen-

\* This work was supported by National Institutes of Health Grants DK065161, P30 DK072506, and P50 DK54690 and by Cystic Fibrosis Foundation Grant R883CR02. The costs of publication of this article were defrayed in part by the payment of page charges. This article must therefore be hereby marked “advertisement” in accordance with 18 U.S.C. Section 1734 solely to indicate this fact.

<sup>1</sup> These authors contributed equally to this work.

<sup>2</sup> To whom correspondence should be addressed: Renal-Electrolyte Division, University of Pittsburgh, 5933 Scaife Hall, 3550 Terrace St., Pittsburgh, PA 15261. Tel.: 412-383-8949; Fax: 412-383-8956; E-mail: hughey@dom.pitt.edu.

<sup>3</sup> The abbreviations used are: ENaC, epithelial Na<sup>+</sup> channel; MDCK, Madin-Darby canine kidney; CCD, cortical collecting duct;  $\gamma$ -43, a synthetic 43 residue peptide derived from the  $\gamma$  subunit; CI, 95% confidence interval.

erated in pcDNA3.1 (+) (Invitrogen) using a standard two-step PCR method. A cDNA clone (IMAGE 3600399) encoding full-length mouse prostasin was obtained from Open Biosystems (Huntsville, AL) and subcloned into pcDNA3.1 (+).

MDCK type 1 cells were a gift from Barry M. Gumbiner (Memorial Sloan-Kettering Cancer Center, New York) and were cultured as previously described (26). Cortical collecting duct (CCDs) cells (mpkCCD<sub>c14</sub>) cells were a gift from Alain Vandewalle (INSERM, Paris, France) and were cultured as previously described (27). Human airway epithelial cells were isolated and cultured as described (28).

**Transient Transfection and Immunoblot Analysis of MDCK Cells**—MDCK cells were transiently transfected with mouse ENaC cDNAs using Lipofectamine 2000 as described by the manufacturer (Invitrogen). The  $\alpha$  and  $\beta$  subunits were carboxyl-terminal epitope-tagged with Myc and FLAG, respectively. The  $\gamma$  subunit (wild type or mutant) had amino-terminal hemagglutinin and carboxyl-terminal V5 epitope tags. Where indicated, mouse prostasin cDNA was co-transfected. The total amount of DNA transfected was held constant by co-transfection of a green fluorescent protein plasmid. Twenty-four hours post-transfection, cells were lysed, and the  $\gamma$  subunit was immunoprecipitated and immunoblotted as described previously (24).

**Biotinylation of Cell-surface Proteins in *Xenopus* Oocytes**—Biotinylation was performed essentially as described by Harris *et al.* (29). All steps were performed on ice using ice-cold solutions. Twenty-four hours post-injection, oocytes (20–40 per group) were placed in an ice-cold modified Barth's saline (MBS; 88 mM NaCl, 1 mM KCl, 2.4 mM NaHCO<sub>3</sub>, 15 mM HEPES, 0.3 mM Ca(NO<sub>3</sub>)<sub>2</sub>, 0.41 mM CaCl<sub>2</sub>, and 0.82 mM MgSO<sub>4</sub>, pH 7.4) lacking antibiotics. After a 30-min incubation, oocytes were washed 4 times with MBS without antibiotics and two times with biotinylation buffer (10 mM triethanolamine, 150 mM NaCl, 2 mM CaCl<sub>2</sub>, pH 9.5). Oocytes were then incubated in biotinylation buffer containing 1 mg/ml EZ-link sulfo-NHS-SS-Biotin (Pierce) for 15 min. Excess biotin reagent was quenched by two washes with quench buffer (192 mM glycine added to MBS) followed by a 5-min incubation in quench buffer. After two washes with MBS, oocytes were lysed by repeated pipetting in lysis buffer (1% Triton X-100, 500 mM NaCl, 5 mM EDTA, 50 mM Tris, pH 7.4) supplemented with 1% (v/v) Protease Inhibitor Mixture III (Pierce). Lysates were centrifuged at 10,000  $\times$  *g* for 10 min, and supernatants were incubated overnight at 4 °C with 50  $\mu$ l of immunopure immobilized streptavidin beads (Pierce) with end-over-end rotation. Beads were then washed three times with lysis buffer and immunoblotted as previously described (24).

**Functional Expression in *Xenopus* Oocytes**—ENaC expression in *Xenopus* oocytes and two-electrode voltage clamp were performed as previously reported (10, 30, 31). Wild type  $\alpha$  and  $\beta$  along with double-tagged  $\gamma$  mouse ENaC cRNAs (1 ng per subunit) were injected with or without 3 ng of mouse prostasin cRNA. Electrophysiological measurements were performed 24 h post-injection. The difference in measured current at –100 mV in the absence and presence of amiloride (10–20  $\mu$ M) was used to identify ENaC-mediated currents.

**Single Channel Studies**—Patch clamp experiments were performed as previously described (32). Single channel currents were acquired at 5 kHz and filtered at 1 kHz by a 4-pole low pass

Bessel filter. For display and analysis, single channel currents were further filtered at 100–200 Hz with a Gaussian filter. Single channel experiments in oocytes were performed in the cell-attached configuration of patch clamp with identical bath and pipette solutions containing 110 mM LiCl, 2 mM CaCl<sub>2</sub>, 1.54 mM KCl, and 10 mM Hepes, pH 7.4. The bath electrode consisted of an Ag-AgCl pellet connected to the bathing solution via an agar bridge made up in 200 mM NaCl. Liquid junction potentials were not corrected. Open probabilities were determined from recordings of at least 6 min in duration at an applied pipette potential of 60 mV. To estimate open probabilities, all point histograms were fit with Gaussian functions using pCLAMP 6 (Axon Instruments, Foster City, CA).

**Peptides**—Peptides were synthesized and high performance liquid chromatography-purified by the peptide synthesis facility of the University of Pittsburgh's Molecular Medicine Institute. The sequences of the peptides in single letter amino acid code were:  $\gamma$  cleavage product ( $\gamma$ -43), EAGSMRSTWEGTPPR-FLNLIPLLVFENEKGGKARDFFTGKRK; scrambled peptide, FKGFVKGKEALREILTFWLRFNNTMDSKPLRTRANPPSKGGRE. Both peptides were modified by amino-terminal acetylation and carboxyl-terminal amidation.

**Short Circuit Current Recordings**—Cells cultured on permeable membrane supports and mounted in modified Costar Ussing chambers were continuously short-circuited by a voltage clamp amplifier (Physiologic Instruments, San Diego, CA) as previously described by Butterworth *et al.* (33).

**Statistical Analysis**—Data are presented as the mean  $\pm$  S.E. Significance comparisons between groups were performed with unpaired Student's *t* tests unless otherwise indicated. A *p* value of less than 0.05 was considered statistically different. IC<sub>50</sub> data are presented as the mean with a 95% confidence interval (CI) and were estimated from normalized currents plotted as a function of the peptide concentration fitted with the following equation:

$$y = b + (t - b)/(1 + 10^{(\log IC_{50} - x)^n}) \quad (\text{Eq. 1})$$

where *y* is the response variable, *x* is the log of the concentration of peptide, *n* is the Hill coefficient, and IC<sub>50</sub> is the concentration of peptide that provokes a response half way between base line (*b*) and maximum response (*t*). Fitting and statistical comparisons were performed with Sigmaplot 8.02 (SPSS Inc, Chicago, IL), GraphPad 3.0 (GraphPad Software, San Diego, CA), and Clampfit 9.0 (Axon Instruments Inc., Union City, CA).

## RESULTS

We recently demonstrated that the  $\alpha$  subunit of ENaC must be cleaved twice at two furin cleavage consensus sites to activate the channel (8–10). This double cleavage event excises a 26-mer inhibitory peptide (10). The  $\gamma$  subunit is cleaved once by furin at a site that aligns closely to the first  $\alpha$  subunit furin site (Fig. 1). Carboxyl-terminal to the single  $\gamma$  subunit furin site is a tetrabasic tract (RKRR<sup>186</sup>) that does not fit the consensus cleavage sequence for furin (34). This sequence may serve as a site for proteolysis by other serine proteases that cleave after basic residues. Prostasin is a serine protease that has been previously shown to activate ENaC when co-expressed in heterologous

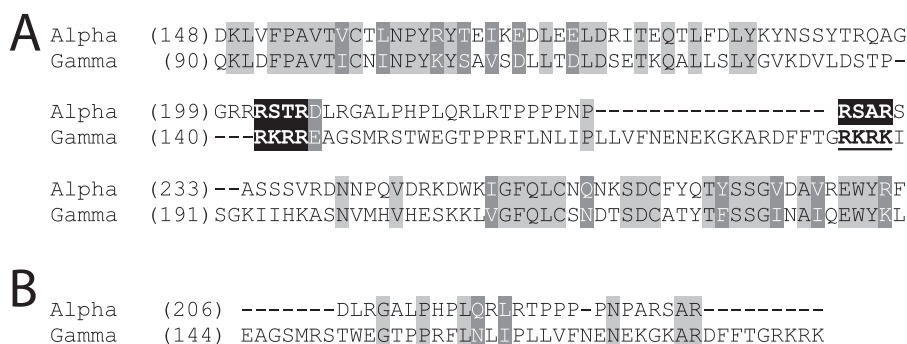


FIGURE 1. **Partial alignment of the mouse ENaC  $\alpha$  and  $\gamma$  subunits.** A, identical residues are highlighted in light gray with black lettering, whereas homologous residues are highlighted in dark gray with white lettering. Furin cleavage sites are highlighted in black, and a tetrabasic tract in the  $\gamma$  subunit is underlined and bolded. B, alternative alignment of peptides released from the  $\alpha$  and  $\gamma$  subunits by proteolytic cleavage.

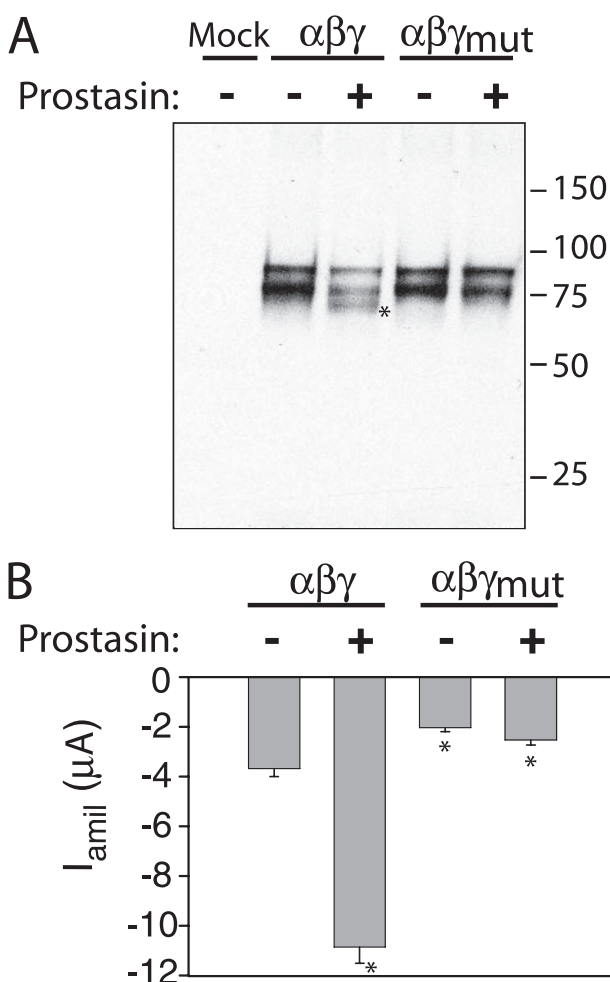


FIGURE 2. **Proastin co-expression activates ENaC by inducing cleavage of the  $\gamma$  subunit.** A, extracts of MDCK cells transiently transfected with epitope-tagged ENaC and with (+) or without (-) proastin were incubated overnight with anti-V5 antibody conjugated to agarose beads. Immunoprecipitates were analyzed by immunoblotting for the V5-tagged  $\gamma$  subunit after SDS-PAGE. Note that co-expression of ENaC with proastin produces a smaller fragment of the  $\gamma$  subunit (see the asterisk) that is absent for the R183Q/K184Q/R185Q/K186Q mutant ( $\gamma_{mut}$ ). Numbers to the right of the gel represent the mobility of Bio-Rad Precision Plus protein standards in kDa. A representative immunoblot is shown ( $n = 3$ ). B, *Xenopus* oocytes were co-injected with cRNAs encoding mouse  $\alpha\beta\gamma$  or  $\alpha\beta\gamma_{mut}$  ENaC with (+) or without (-) proastin. Whole cell amiloride-sensitive currents were measured the following day at a clamp potential of  $-100$  mV ( $n = 28-30$ ). \*,  $p < 0.005$  compared with  $\alpha\beta\gamma$  without proastin ( $n = 28-30$ ).

systems (13–15, 20). Previous studies suggest that a tetra-basic (or dibasic) tract could serve as a substrate for proastin cleavage (35). We, therefore, examined whether co-expression of ENaC and proastin altered proteolysis of the  $\gamma$  subunit. ENaCs were expressed in MDCK cells with the  $\gamma$  subunit bearing a carboxyl-terminal V5 epitope tag. After cell lysis, immunoprecipitation, and subsequent immunoblotting with an anti-V5 antibody, we observed both full-length (93 kDa) and furin-cleaved (75 kDa)  $\gamma$  subunit (Fig. 2A). When

ENaCs were co-expressed with proastin, an additional  $\gamma$  subunit species of 70 kDa was observed, consistent with cleavage at a site carboxyl-terminal to the furin cleavage site. When the RKRK<sup>186</sup> tract in the  $\gamma$  subunit was mutated to QQQQ<sup>186</sup> ( $\gamma_{mut}$ ), only the full-length and 75 kDa fragments were observed both in the absence and presence of proastin expression. These data suggest that proastin induces cleavage of the  $\gamma$  subunit at the RKRK<sup>186</sup> tract.

Co-expression of ENaC and proastin led to a significant, 3-fold increase in whole cell amiloride-sensitive Na<sup>+</sup> currents in *Xenopus* oocytes compared with oocytes expressing ENaC alone (Fig. 2B). Expression of channels with the  $\gamma$  subunit R183Q/K184Q/R185Q/K186Q mutation led to a significant 45% reduction in whole cell Na<sup>+</sup> currents compared with oocytes expressing wild type ENaCs. Furthermore, co-expression of this mutant ENaC with proastin led to only a modest, but non-significant increase in Na<sup>+</sup> currents when compared with oocytes expressing the mutant channels alone ( $p > 0.05$ ). These results suggest that proastin-induced cleavage at the RKRK<sup>186</sup> site plays a major role in proastin-dependent activation of ENaC.

Previous reports based on a cell surface expression assay in *Xenopus* oocytes have inferred that proastin induces activation of ENaC through an increase in single channel open probability (13–15). We examined the open probability of wild type ENaCs expressed in *Xenopus* oocytes with or without proastin co-expression. In contrast to the observations of Adachi *et al.* (20), channel open probability increased 89% from  $0.46 \pm 0.05$  ( $n = 11$ ) to  $0.87 \pm 0.04$  ( $n = 7$ ,  $p < 0.0001$ ) when ENaC was co-expressed with proastin (Fig. 3). Proastin co-expression had no effect on unitary currents at an applied pipette potential of  $+60$  mV ( $0.41 \pm 0.01$  pA versus  $0.39 \pm 0.01$  pA,  $p = 0.33$ ).

We have recently reported that cleavage of ENaC at two sites within the  $\alpha$  subunit activates the channel by releasing an inhibitory 26-mer peptide (10). We, therefore, sought to determine whether the 43-mer tract in the  $\gamma$  subunit (Glu-144–Lys-186), predicted to be excised after co-expression with proastin, also functions as an inhibitory domain. We first examined whether deletion of the 43-mer tract in the  $\gamma$  subunit would enhance channel activity. In addition to removing the tract, Arg-143 within the  $\gamma$  furin site was mutated to Ala to prevent furin-dependent cleavage. This mutant  $\gamma$ R143A, $\Delta$ 144–186 ( $\gamma$ R/ $\Delta$ )

## ENaC Activation by Prostasin

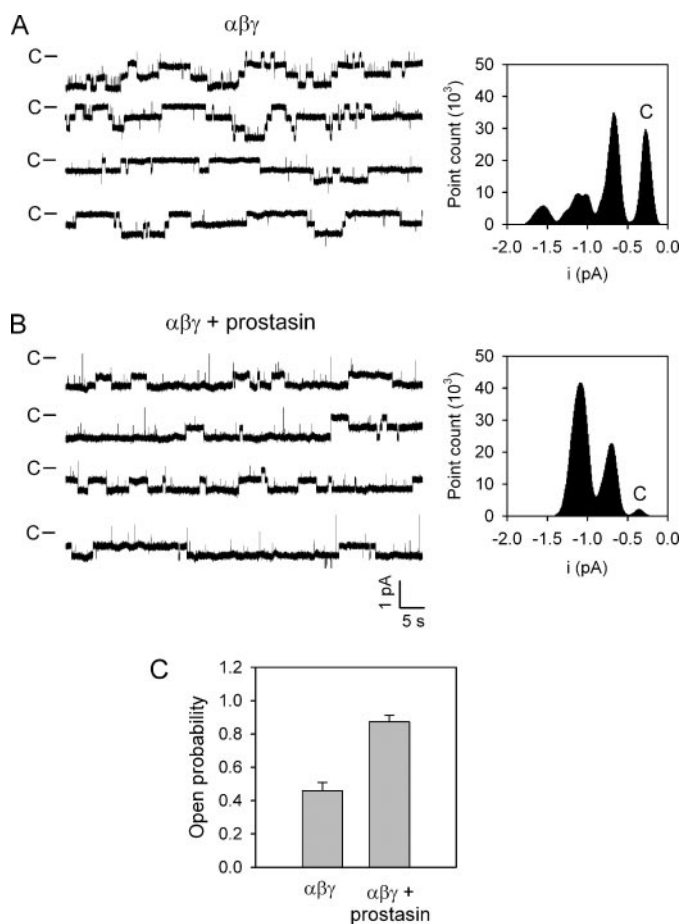


**FIGURE 3. Prostasin increases the open probability of ENaC.** Single channel recordings were performed in the cell-attached configuration of patch clamp using oocytes co-expressing wild type ENaC with or without prostasin as described under "Experimental Procedures." Representative single channel recordings from oocytes expressing wild type channels with (B) or without (A) prostasin are shown. Amplitude histograms are presented at the right side of each recording. C indicates the closed state. C, open probabilities of ENaC estimated from oocytes co-expressing wild type channels with or without prostasin in the same batch of oocytes ( $n = 7-11$ ,  $p < 0.0001$ , unpaired Student's  $t$  test).

was not cleaved when co-expressed with  $\alpha$  and  $\beta$  subunits in MDCK cells (Fig. 4B). However, when this mutant was co-expressed with  $\alpha$  and  $\beta$  subunits in oocytes, whole cell  $\text{Na}^+$  currents were 3.7-fold greater than currents recorded in oocytes expressing wild type  $\alpha\beta\gamma$  (Fig. 4A). At a single channel level, the mutant channel was constitutively active, with an open probability of  $>0.95$ , compared with wild type channels that had an open probability of  $0.37 \pm 0.06$  (Fig. 5). Unitary currents were not different between mutant ( $0.39 \pm 0.03$  pA) and wild type ( $0.40 \pm 0.01$ ) channels at an applied pipette potential of  $+60$  mV ( $n = 4$ ,  $p = 0.75$ ).

Our results suggest that cleavage of the  $\gamma$  subunit by furin and prostasin is required to release an inhibitory domain. If this hypothesis is correct, mutation of the  $\gamma$  furin site to block furin cleavage should prevent prostasin-dependent activation of the channel. Indeed, we observed that  $\alpha\beta\gamma\text{R143A}$ , a mutant that lacks furin-dependent proteolysis of the  $\gamma$  subunit (8), was not activated by prostasin when co-expressed in oocytes (Fig. 6).

We next examined whether a synthetic peptide ( $\gamma$ -43), corresponding to the 43-mer tract excised from the  $\gamma$  subunit,

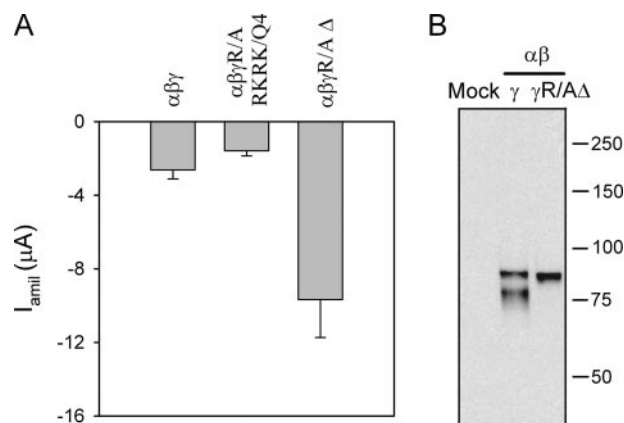


**FIGURE 4. The tract  $\gamma\text{Glu-144-Lys-186}$  inhibits channel activity.** Either wild type or mutant ENaCs were expressed in oocytes and MDCK cells. The  $\gamma$  subunit had amino-terminal hemagglutinin and carboxyl-terminal V5 epitope tags. A, deletion of the tract  $\gamma\text{Glu-144-Lys-186}$  ( $\Delta$ 144-186) between both the furin and prostasin consensus cleavage sites increased ENaC activity. Amiloride-sensitive whole cell currents were significantly different between oocytes expressing  $\alpha\beta\gamma$  versus  $\alpha\beta\gamma\text{R143A,RKRK/Q4}$  ( $\gamma\beta\gamma\text{R/A}$ ,  $RKRK/Q4$ ) ( $p < 0.05$ ) or  $\alpha\beta\gamma\text{R143A},\Delta$ 144-186 ( $\alpha\beta\gamma\text{R/A}\Delta$ ) channels ( $p < 0.001$ , Kruskal Wallis test (nonparametric analysis of variance) followed by Dunn's multiple comparisons post-test,  $n = 16$ ). B, characterization of  $\gamma$ -subunit processing in MDCK cells. ENaC was immunoprecipitated with anti-V5 antibodies from extracts of MDCK cells transiently expressing wild type  $\alpha\beta\gamma$  or  $\alpha\beta\gamma\text{R143A},\Delta$ 144-186. After SDS-PAGE, the immunoprecipitates were blotted for the V5-tagged  $\gamma$  subunit. Numbers to the right of the gel represent the mobility of Bio-Rad Precision Plus protein standards in kDa. A representative immunoblot is shown ( $n = 3$ ).

inhibited endogenous ENaC in epithelia. When added to the apical chamber of filter grown mouse CCD cells,  $\gamma$ -43 ( $3 \mu\text{M}$ ) rapidly inhibited short circuit currents (Fig. 7A). Peptide-dependent inhibition of the channel was reversible as the current was restored after washout of  $\gamma$ -43. This peptide inhibited short circuit currents in mouse CCD cells and in primary cultures of human airway cells in a dose-dependent manner, with an  $\text{IC}_{50}$  of  $3.2 \mu\text{M}$  (CI,  $2.7-3.8 \mu\text{M}$ ) and  $2.0 \mu\text{M}$  (CI,  $1.9-2.2 \mu\text{M}$ ), respectively (Fig. 7, B and C) ( $n = 8-9$ ). In contrast, a minimal effect on short circuit current was observed upon the addition of a control, scrambled peptide. These data suggest that the 43-mer tract excised by furin- and prostasin-dependent proteolysis functions as an endogenous inhibitor of ENaC activity prior to  $\gamma$  subunit cleavage.

We recently reported that the inhibitory 26-mer peptide cleaved from the  $\alpha$  subunit does not appear to interact with the amiloride binding site, based on its lack of competition with amiloride (10). To our surprise, the  $\gamma$ -43 peptide significantly increased the  $\text{IC}_{50}$  for amiloride block by 60% in CCD cells (Fig. 8). The amiloride  $\text{IC}_{50}$  was  $431$  nM (CI,  $339-548$  nM) in the presence of  $3 \mu\text{M}$   $\gamma$ -43 and  $270$  nM (CI,  $238-306$  nM) in the absence of  $\gamma$ -43.

The role of prostasin catalytic activity in ENaC activation has recently been called into question. Although the serine protease inhibitor aprotinin abolishes prostasin-induced activation of ENaC in *Xenopus* oocytes (13-15, 20), mutations within the prostasin putative catalytic triad do not prevent this activation (36). We, therefore, examined whether a catalytic site mutant of prostasin could activate ENaC as well as induce cleavage of the  $\gamma$  subunit. Co-expression of a prostasin mutant S238A (within the catalytic triad) and  $\alpha\beta\gamma$  in oocytes resulted in a significant increase in whole cell  $\text{Na}^+$  currents compared with *Xenopus*

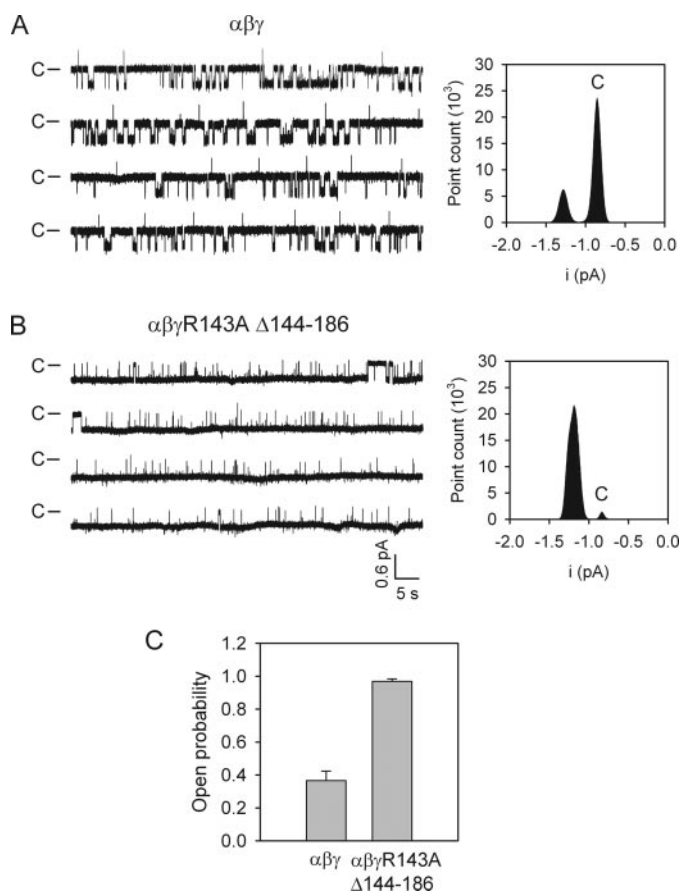


**FIGURE 5. Deletion of the tract  $\gamma$ Glu-144-Lys-186 increases ENaC single channel open probability.** Single channel recordings were performed in the cell-attached configuration of patch clamp from oocytes expressing wild type  $\alpha\beta\gamma$  or  $\alpha\beta\gamma$ R143A, $\Delta$ 144–186 as described under “Experimental Procedures.” Representative single channel recordings of wild type  $\alpha\beta\gamma$  (A) or  $\alpha\beta\gamma$ R143A, $\Delta$ 144–186 (B) channels are shown. Amplitude histograms are presented at the right side of each recording. C indicates the closed state. C, open probabilities were statistically different in oocytes expressing wild type  $\alpha\beta\gamma$  and  $\alpha\beta\gamma$ R143A, $\Delta$ 144–186 channels ( $p < 0.005$ , unpaired Student’s *t* test with Welch correction,  $n = 4$ ).

oocytes expressing only wild type  $\alpha\beta\gamma$  (Fig. 9A). However, this prostin mutant did not activate  $\alpha\beta\gamma_{mut}$  (R183Q/K184Q/R185Q/K186Q) channels, suggesting that prostin S238A enhanced cleavage of the  $\gamma$  subunit at a site distal to the furin cleavage site (presumably at the RKRK<sup>186</sup> site). We examined proteolytic processing of  $\gamma$  subunits at the surface of oocytes expressing either  $\alpha\beta\gamma$  alone, co-expressing  $\alpha\beta\gamma$  and prostin, or co-expressing  $\alpha\beta\gamma$  and prostin S238A. Both the full-length (93 kDa)  $\gamma$  subunit and a furin-processed 80-kDa carboxyl-terminal  $\gamma$  subunit fragment were observed in oocytes expressing ENaC alone, in agreement with our previously published findings (8). Both full-length and a presumably prostin-processed 75-kDa  $\gamma$  subunits were observed in oocytes co-expressing  $\alpha\beta\gamma$  and prostin. The full-length (93 kDa)  $\gamma$  subunit and the cleaved 80- and 75-kDa  $\gamma$  subunits were observed in oocytes co-expressing  $\alpha\beta\gamma$  and the prostin S238A mutant (Fig. 9B). These data suggest that prostin S238A induces cleavage of the  $\gamma$  subunit at a site distal to the furin cleavage site, although the apparent efficiency of prostin S238A-induced  $\gamma$  subunit processing is less than that observed with wild type prostin. When expressed in oocytes, the cleaved  $\gamma$  subunits appeared to

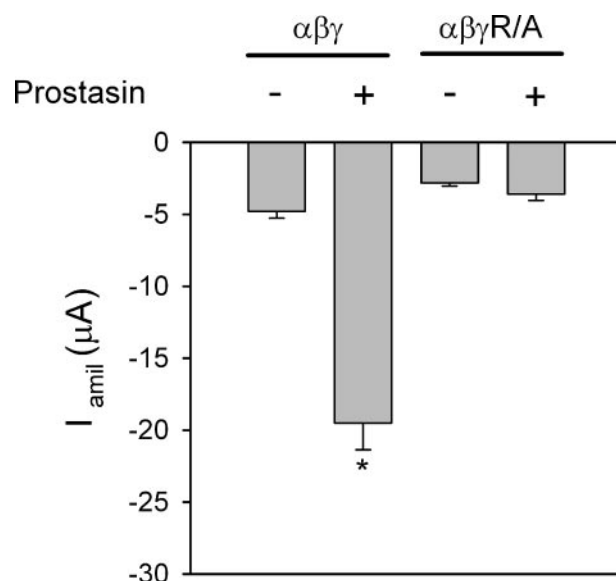


**FIGURE 6. Prostin does not activate  $\alpha\beta\gamma$ R143A channels that lack furin-dependent cleavage of  $\gamma$ .** Xenopus oocytes were co-injected with cRNAs encoding  $\alpha\beta\gamma$  or  $\alpha\beta\gamma$ R143A with (+) or without (–) prostin. Whole cell amiloride (*amil*)-sensitive currents were measured the following day at a clamp potential of  $-100$  mV. \*,  $p < 0.001$  compared with  $\alpha\beta\gamma$  without prostin (Kruskal Wallis test (nonparametric analysis of variance) followed by Dunn’s multiple comparisons post-test,  $n = 20$ ).

migrate slower by SDS-PAGE than when expressed in MDCK cells (Fig. 2A). These differences in apparent molecular weights likely reflect differences in Asn-linked glycan terminal processing.

## DISCUSSION

We previously reported that ENaC  $\alpha$  and  $\gamma$  subunits are processed by the endoprotease furin within their extracellular domains (8). Two extracellular furin cleavage sites are present within the  $\alpha$  subunit, and inhibition of furin-dependent processing of the  $\alpha$  subunit by mutating either one or both furin cleavage sites led to a profound inhibition of ENaC activity (8–10). Furin-dependent cleavage of the  $\alpha$  subunit releases a 26-mer inhibitory peptide (10). We have also shown that the  $\gamma$  subunit is cleaved once by furin. In contrast to the  $\alpha$  subunit, prevention of furin-dependent processing of the  $\gamma$  subunit was associated with only a modest reduction in ENaC activity (8).

Our observation that the  $\alpha$  subunit must be cleaved twice to activate ENaC raised the possibility that the  $\gamma$  subunit also must be cleaved twice to fully activate ENaC by releasing a second inhibitory peptide. Because there is only one furin cleavage site in the  $\gamma$  subunit, other proteases might cleave the  $\gamma$  subunit and activate ENaC. Our results suggest that prostin or a subsequent protease activated by prostin fulfills this task. Prostin cleavage occurs immediately after tracts of basic amino acid residues (35). We identified an RKRK<sup>186</sup> tract  $\sim$ 40 residues carboxyl-terminal to the furin cleavage site in the  $\gamma$  subunit as a potential prostin-dependent cleavage site. Several lines of evidence suggest that prostin is responsible for  $\gamma$  subunit cleavage at this site. Co-expression of ENaC and prostin in MDCK cells and *Xenopus* oocytes resulted in the appearance of a second, more rapidly migrating  $\gamma$  subunit cleavage product, consistent with the expected change in mobility upon cleavage

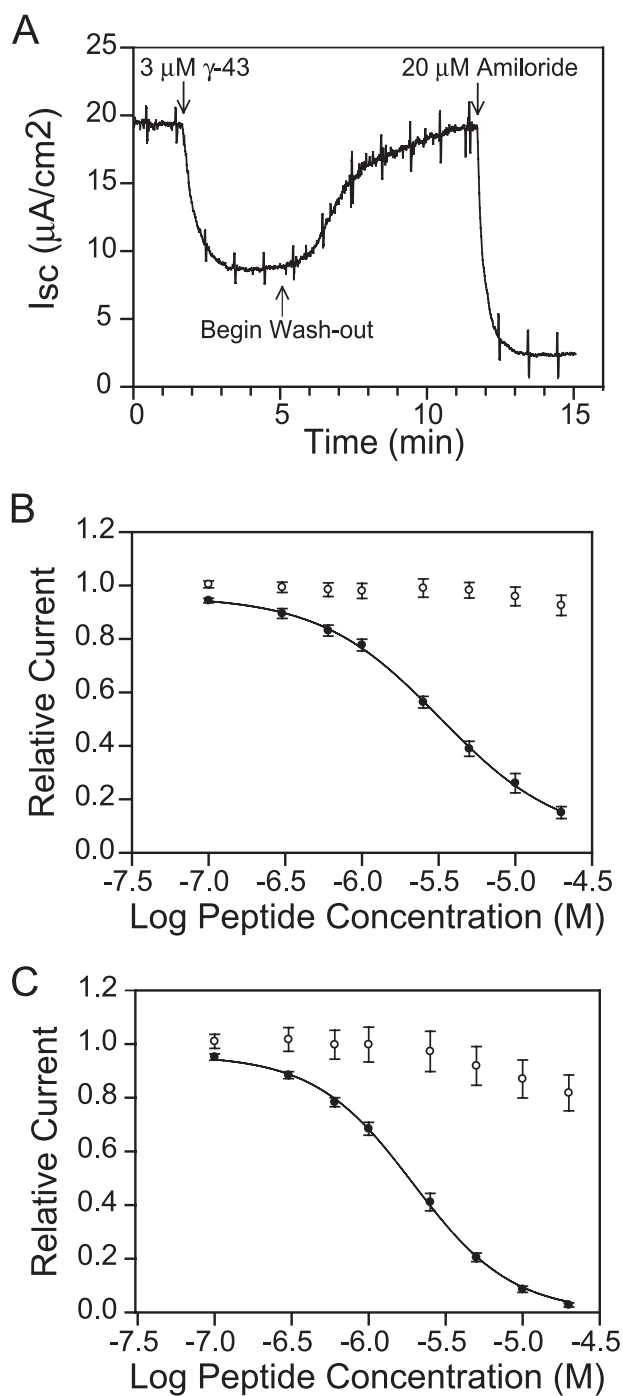


**FIGURE 7. A peptide ( $\gamma$ -43) representing the  $\gamma$  cleavage product inhibits transepithelial  $\text{Na}^+$  transport in epithelia endogenously expressing ENaC.** *A*, mouse CCD cells cultured on permeable membrane supports and mounted in a modified Ussing chamber were continuously short-circuited. Transepithelial resistance was monitored by applying a 4-mV bipolar pulse every 60 s. Where indicated, a 43-residue peptide corresponding to the tract Glu-144–Lys-186 of mouse  $\gamma$  ENaC ( $\gamma$ -43) was added to the apical chamber at a final concentration of  $3 \mu\text{M}$ . This led to a marked inhibition of transepithelial  $\text{Na}^+$  transport that was relieved by washout of the peptide. Subsequent application of  $20 \mu\text{M}$  amiloride to the apical chamber confirmed that the short circuit current reflected ENaC-mediated transepithelial  $\text{Na}^+$  transport. Tracing is representative of five experiments. CCD cells (*B*) or primary cultures of human airway cells (*C*) cultured and voltage-clamped as above were exposed to increasing concentrations of either  $\gamma$ -43 (filled circles) or a scrambled peptide (open circles). Although the scrambled peptide failed to inhibit amiloride-sensitive short circuit currents, the  $\gamma$  cleavage product inhibited in a dose-dependent manner ( $n = 8$ – $9$ ).  $I_{sc}$  short circuit current.

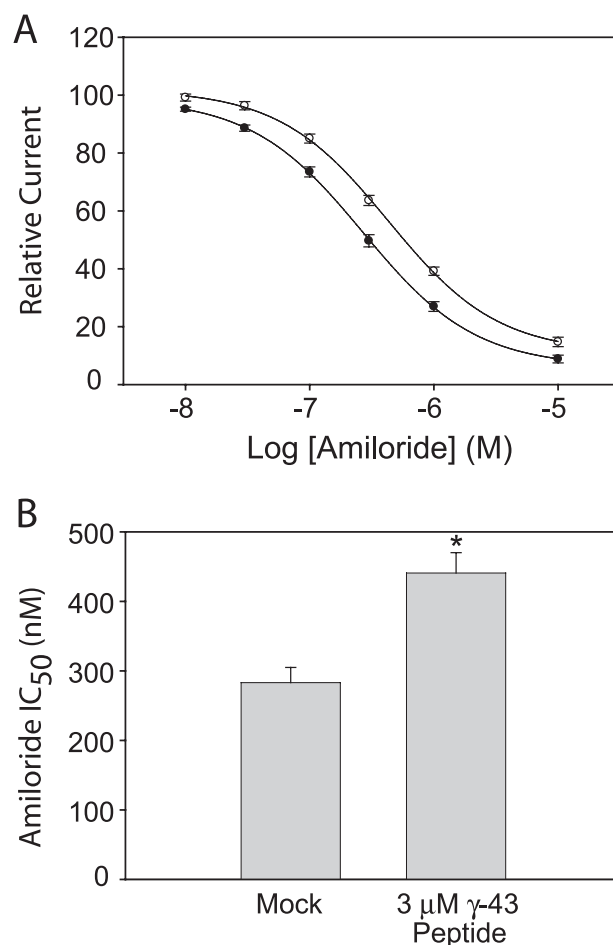


**FIGURE 8. Effect of the  $\gamma$ -43 peptide on amiloride block of ENaC.** Mouse CCD cells cultured on permeable membrane supports and mounted in a modified Ussing chamber were continuously short-circuited by a voltage clamp amplifier (Physiologic Instruments, San Diego, CA). *A*, dose response curves for amiloride in the presence (open circles) or absence (closed circles) of  $3 \mu\text{M}$   $\gamma$ -43 peptide. *B*, amiloride  $\text{IC}_{50}$  values in the absence or presence of  $3 \mu\text{M}$   $\gamma$ -43 peptide ( $n = 18$ ).  $*$ ,  $p < 0.001$ .

at the RKRK<sup>186</sup> site (Fig. 2*A* and 9*B*). This second cleavage product was absent when proastasin was co-expressed with a mutant ENaC where the residues in the RKRK<sup>186</sup> tract were changed to glutamine. Moreover, when this mutant ENaC was expressed in *Xenopus* oocytes, co-expression of proastasin failed to significantly activate ENaC, whereas this protease enhanced the activity of wild type ENaC (Fig. 2*B*). The fact that channels with the  $\gamma$  subunit R183Q/K184Q/R185Q/K186Q mutation exhibited lower currents than wild type channels suggests that there may be limited proteolysis of wild type channels at this site in *Xenopus* oocytes in the absence of proastasin co-expression.

If proastasin and furin activate ENaC as a result of two separate cleavage events in the  $\gamma$  subunit that releases a 43-mer inhibitory peptide, we reasoned that channels lacking this tract would exhibit an increase in channel activity. We found that channels lacking both this 43-mer tract and the furin cleavage site in the  $\gamma$  subunit exhibited greatly enhanced activity (Fig. 4*A*) and an open probability that approached 1.0 (Fig. 5) even though this mutant  $\gamma$  subunit was not cleaved (Fig. 4*B*). The synthetic 43-mer peptide  $\gamma$ -43 reversibly inhibited endogenous

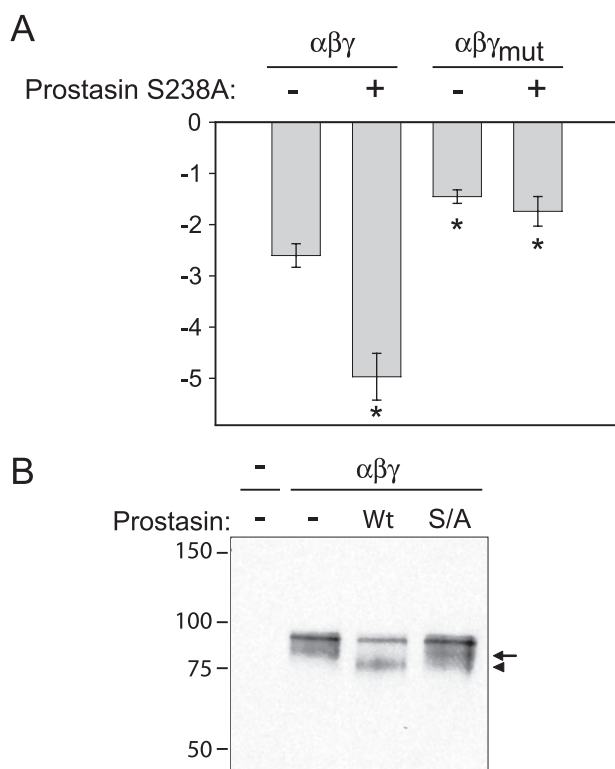


**FIGURE 9. Activation of ENaC by a catalytic site mutant of proastasin also requires the  $\gamma$  subunit RKRK<sup>186</sup> tract.** *A*, *Xenopus* oocytes were injected with cRNAs encoding mouse  $\alpha\beta\gamma$  or  $\alpha\beta\gamma_{mut}$  ( $\gamma$ R183Q/K184Q/R185Q/K186Q) ENaC with (+) or without (-) the S238A mutant (S/A) proastasin. Whole cell amiloride-sensitive currents ( $\mu A$ ) were measured the following day at a clamp potential of  $-100$  mV ( $n = 21$ ). \*,  $p < 0.05$  compared with  $\alpha\beta\gamma$  without proastasin S238A. *B*, streptavidin precipitates of biotinylated oocyte surface proteins were analyzed by immunoblotting with an anti-V5 antibody after SDS-PAGE. Note that co-expression of ENaC with both wild type (Wt) and S238A proastasin produced a fragment of the  $\gamma$  subunit (arrowhead) that is smaller than the  $\gamma$  subunit furin cleavage product (arrow). Numbers to the left of the gel represent the mobility of Bio-Rad Precision Plus protein standards. A representative immunoblot is shown ( $n = 2$ ).

ENaCs expressed in human airway epithelial cells and in mouse CCD cells with  $IC_{50}$  values of  $\sim 2$ – $3$   $\mu M$  (Fig. 7). We also reasoned that channels lacking furin processing of the  $\gamma$  subunit ( $\alpha\beta\gamma$ R143A) would not be activated by proastasin due to lack of release of an inhibitory domain. Indeed, this is what we observed (Fig. 6).

Although peptides excised from both the  $\alpha$  and  $\gamma$  subunits inhibit ENaCs, they share limited similarity at the primary amino acid level (Fig. 1B). There are a number of other differences between these two inhibitory peptides. The 43-mer  $\gamma$  subunit derived peptide is a relatively potent inhibitor of ENaC expressed in human airway and mouse CCD cells (Fig. 7), in contrast to the 26-mer peptide derived from  $\alpha$  subunit cleavage that inhibited ENaC activity in human airway and mouse CCD cells with  $IC_{50}$  values of  $50$ – $100$   $\mu M$  (10). The  $\alpha$  subunit-derived peptide did not alter the  $IC_{50}$  of amiloride for ENaC, suggesting that the 26-mer peptide and amiloride interact at distinct sites within ENaC (10). In contrast, the  $\gamma$  subunit-derived peptide  $\gamma$ -43 significantly altered the dose-dependent inhibition of amiloride (Fig. 8). Although the  $\gamma$ -43 peptide and amiloride may interact at common sites within the channel (competitive inhibition), the modest change in the apparent amiloride  $IC_{50}$  in the presence of  $\gamma$ -43 peptide is also consistent with amiloride

and the  $\gamma$ -43 peptide interacting at distinct sites (non-competitive inhibition). Binding of the peptide to the channel may indirectly affect amiloride binding.

Previous studies demonstrating that the serine protease inhibitor aprotinin abolishes proastasin-induced activation of ENaC in *Xenopus* oocytes (13–15, 20) are consistent with the possibility that proastasin activates ENaC by cleaving the  $\gamma$  subunit. However, the role of proastasin catalytic activity in ENaC activation has recently been called into question. Serine proteases have three well defined residues, referred to as a catalytic triad, which are required for catalytic activity (37). Andreasen *et al.* (36) recently reported that proastasin with mutations within its putative catalytic triad activates ENaC when co-expressed in oocytes.

We confirmed that proastasin bearing a mutation of one of the catalytic triad residues (S238A) activates ENaC expressed in oocytes (Fig. 9A). This proastasin mutant did not activate ENaCs with the  $\gamma$  subunit mutation R183Q/K184Q/R185Q/K186Q at the putative proastasin cleavage site (Fig. 9). Surprisingly, channel activation by this mutant proastasin was associated with proteolytic processing of the  $\gamma$  subunit. The more rapidly migrating  $\gamma$  subunit cleavage product (75 kDa) was readily detected when wild type ENaC was co-expressed with the S238A proastasin mutant in oocytes (Fig. 9B), suggesting that this proastasin mutant induces cleavage of the  $\gamma$  subunit at the RKRK<sup>186</sup> site. The catalytic activity of proastasin bearing mutations within the putative catalytic triad has not previously been addressed. However, Carter and Wells (38) have reported that mutations within the catalytic triad of *Bacillus amyloliquefaciens* subtilisin do not completely eliminate catalytic activity (38). Alternatively, the mutant proastasin as well as wild type proastasin might bind to and suppress endogenous *Xenopus* protease inhibitors, allowing an endogenous protease to cleave the  $\gamma$  subunit within the RKRK<sup>186</sup> tract.

Our results begin to address the question of why multiple proteases have a role in the activation of ENaC. Furin-dependent cleavage of the  $\alpha$  subunit at two sites releases a 26-mer inhibitory peptide (10). However, furin-dependent cleavage of the  $\gamma$  subunit occurs at only one site and is not expected to release the  $\gamma$  subunit inhibitory peptide (8). A second cleavage event mediated by proastasin or perhaps other proteases such as elastase is required to release a  $\gamma$  subunit inhibitory peptide. Harris *et al.* (29) recently reported that exogenous neutrophil elastase cleaves the  $\gamma$  subunit of rat ENaC expressed at the cell surface of *Xenopus* oocytes and increases  $I_{Na}$  by 5–7-fold.

We propose that multiple proteolytic cleavage events lead to a stepwise activation of ENaC, reflected in a stepwise increase in channel open probability. Channels that lack proteolytic processing have a low open probability (9). Channels that have been cleaved solely by furin exhibit an intermediate open probability, as these are likely the active channels that are observed in *Xenopus* oocytes at a single channel level (Fig. 3A), where there appears to be limited proteolytic release of the  $\gamma$  subunit inhibitory peptide under basal conditions. In contrast, channels that have released both  $\alpha$  subunit and  $\gamma$  subunit inhibitory peptides exhibit a high open probability, as we observed in oocytes co-expressing ENaC and proastasin (Fig. 3B).

Previous studies in airway epithelial cells and renal cortical collecting duct cells have shown that nonspecific inhibitors of proastasin, such as aprotinin, bikunin, and protease nexin-1 reduce ENaC activity (14–20, 39). Channel activity can be restored by either removing the inhibitor or by treating cells with extracellular trypsin (16–18). In cultured CCD cells, we have also shown that a furin-specific inhibitor ( $\alpha$ 1-PDX) dramatically reduced ENaC activity (8). It has been unclear why inhibitors of both proastasin and furin reduce channel activity. We previously reported that two pools of channels are present at the plasma membrane, a pool of channels processed by furin and perhaps other proteases and a second pool of near silent channels that have escaped proteolytic processing (40). We and others have suggested that these non-cleaved channels represent a pool of nearly silent channels and that proastasin or other proteases might activate ENaC by processing these non-cleaved channels at the plasma membrane (40–42). Mechanisms by which proastasin activates ENaC are clearly more complex. In addition to the processing of non-cleaved channels, proastasin-dependent processing of channels that have been already cleaved by furin in the biosynthetic pathway further enhances channel activity.

In summary, our results suggest that proastasin activates ENaC by affecting cleavage of the  $\gamma$  subunit and, in concert with furin-dependent cleavage of the  $\gamma$  subunit, releases an inhibitory peptide. In a similar manner, furin-dependent processing within the  $\alpha$  subunit at two sites releases an inhibitory peptide. These peptides released from the  $\alpha$  and  $\gamma$  subunits may serve as initial templates for developing a new class of peptide based ENaC inhibitors.

*Acknowledgments*—The mpkCCD<sub>c14</sub> cells were a gift from Alain Vandewalle (Paris, France). MDCK cells were a gift from Barry Gumbiner (Memorial Sloan-Kettering Cancer Center, New York).

## REFERENCES

- Snyder, P. M., McDonald, F. J., Stokes, J. B., and Welsh, M. J. (1994) *J. Biol. Chem.* **269**, 24379–24383
- Renard, S., Lingueglia, E., Voilley, N., Lazdunski, M., and Barbry, P. (1994) *J. Biol. Chem.* **269**, 12981–12986
- Canessa, C. M., Merillat, A. M., and Rossier, B. C. (1994) *Am. J. Physiol.* **267**, C1682–C1690
- Schild, L., Schneeberger, E., Gautschi, I., and Firsov, D. (1997) *J. Gen. Physiol.* **109**, 15–26
- Snyder, P. M., Olson, D. R., and Bucher, D. B. (1999) *J. Biol. Chem.* **274**, 28484–28490
- Sheng, S., Li, J., McNulty, K. A., Kieber-Emmons, T., and Kleyman, T. R. (2001) *J. Biol. Chem.* **276**, 1326–1334
- Sheng, S., McNulty, K. A., Harvey, J. M., and Kleyman, T. R. (2001) *J. Biol. Chem.* **276**, 44091–44098
- Hughey, R. P., Bruns, J. B., Kinlough, C. L., Harkleroad, K. L., Tong, Q., Carattino, M. D., Johnson, J. P., Stockand, J. D., and Kleyman, T. R. (2004) *J. Biol. Chem.* **279**, 18111–18114
- Sheng, S., Carattino, M. D., Bruns, J. B., Hughey, R. P., and Kleyman, T. R. (2006) *Am. J. Physiol. Renal Physiol.* **290**, 1488–1496
- Carattino, M. D., Sheng, S., Bruns, J. B., Pilewski, J. M., Hughey, R. P., and Kleyman, T. R. (2006) *J. Biol. Chem.* **281**, 18901–18907
- Chraïbi, A., and Horisberger, J. D. (2002) *J. Gen. Physiol.* **120**, 133–145
- Rossier, B. C. (2004) *Proc. Am. Thorac. Soc.* **1**, 4–9
- Vuagniaux, G., Vallet, V., Jaeger, N. F., Hummler, E., and Rossier, B. C. (2002) *J. Gen. Physiol.* **120**, 191–201
- Vallet, V., Chraïbi, A., Gaeggeler, H. P., Horisberger, J. D., and Rossier, B. C. (1997) *Nature* **389**, 607–610
- Vuagniaux, G., Vallet, V., Jaeger, N. F., Pfister, C., Bens, M., Farman, N., Courtois-Coutry, N., Vandewalle, A., Rossier, B. C., and Hummler, E. (2000) *J. Am. Soc. Nephrol.* **11**, 828–834
- Liu, L., Hering-Smith, K. S., Schiro, F. R., and Hamm, L. L. (2002) *Hypertension* **39**, 860–864
- Adebamiro, A., Cheng, Y., Johnson, J. P., and Bridges, R. J. (2005) *J. Gen. Physiol.* **126**, 339–352
- Bridges, R. J., Newton, B. B., Pilewski, J. M., Devor, D. C., Poll, C. T., and Hall, R. L. (2001) *Am. J. Physiol. Lung Cell. Mol. Physiol.* **281**, 16–23
- Myerburg, M. M., Butterworth, M. B., McKenna, E. E., Peters, K. W., Frizzell, R. A., Kleyman, T. R., and Pilewski, J. M. (2006) *J. Biol. Chem.* **281**, 27942–27949
- Adachi, M., Kitamura, K., Miyoshi, T., Narikiyo, T., Iwashita, K., Shiraishi, N., Nonoguchi, H., and Tomita, K. (2001) *J. Am. Soc. Nephrol.* **12**, 1114–1121
- Vallet, V., Pfister, C., Loffing, J., and Rossier, B. C. (2002) *J. Am. Soc. Nephrol.* **13**, 588–594
- Narikiyo, T., Kitamura, K., Adachi, M., Miyoshi, T., Iwashita, K., Shiraishi, N., Nonoguchi, H., Chen, L. M., Chai, K. X., Chao, J., and Tomita, K. (2002) *J. Clin. Investig.* **109**, 401–408
- Iwashita, K., Kitamura, K., Narikiyo, T., Adachi, M., Shiraishi, N., Miyoshi, T., Nagano, J., Tuyen, D. G., Nonoguchi, H., and Tomita, K. (2003) *J. Am. Soc. Nephrol.* **14**, 11–16
- Vallet, V., Pfister, G. M., Bruns, J. B., Kinlough, C. L., Poland, P. A., Harkleroad, K. L., Carattino, M. D., and Kleyman, T. R. (2003) *J. Biol. Chem.* **278**, 37073–37082
- Ahn, Y. J., Brooker, D. R., Kosari, F., Harte, B. J., Li, J., Mackler, S. A., and Kleyman, T. R. (1999) *Am. J. Physiol.* **277**, F121–F129
- Lavelle, J. P., Negrete, H. O., Poland, P. A., Kinlough, C. L., Meyers, S. D., Hughey, R. P., and Zeidel, M. L. (1997) *Am. J. Physiol.* **273**, F67–F75
- Bens, M., Vallet, V., Cluzeaud, F., Pascual-Letallec, L., Kahn, A., Rafestin-Oblin, M. E., Rossier, B. C., and Vandewalle, A. (1999) *J. Am. Soc. Nephrol.* **10**, 923–934
- Devor, D. C., Bridges, R. J., and Pilewski, J. M. (2000) *Am. J. Physiol. Cell Physiol.* **279**, 461–479
- Harris, M., Firsov, D., Vuagniaux, G., Stutts, M. J., and Rossier, B. C. (2007) *J. Biol. Chem.* **282**, 58–64
- Bruns, J. B., Hu, B., Ahn, Y. J., Sheng, S., Hughey, R. P., and Kleyman, T. R. (2003) *Am. J. Physiol. Renal Physiol.* **285**, 600–609
- Carattino, M. D., Hill, W. G., and Kleyman, T. R. (2003) *J. Biol. Chem.* **278**, 36202–36213
- Carattino, M. D., Sheng, S., and Kleyman, T. R. (2005) *J. Biol. Chem.* **280**, 4393–4401
- Butterworth, M. B., Edinger, R. S., Johnson, J. P., and Frizzell, R. A. (2005) *J. Gen. Physiol.* **125**, 81–101
- Rockwell, N. C., Krysan, D. J., Komiyama, T., and Fuller, R. S. (2002) *Chem. Rev.* **102**, 4525–4548
- Shipway, A., Danahay, H., Williams, J. A., Tully, D. C., Backes, B. J., and Harris, J. L. (2004) *Biochem. Biophys. Res. Commun.* **324**, 953–963
- Andreasen, D., Vuagniaux, G., Fowler-Jaeger, N., Hummler, E., and Rossier, B. C. (2006) *J. Am. Soc. Nephrol.* **17**, 968–976
- Dodson, G., and Wlodawer, A. (1998) *Trends Biochem. Sci.* **23**, 347–352
- Carter, P., and Wells, J. A. (1988) *Nature* **332**, 564–568
- Wakida, N., Kitamura, K., Tuyen, D. G., Maekawa, A., Miyoshi, T., Adachi, M., Shiraishi, N., Ko, T., Ha, V., Nonoguchi, H., and Tomita, K. (2006) *Kidney Int.* **70**, 1432–1438
- Hughey, R. P., Bruns, J. B., Kinlough, C. L., and Kleyman, T. R. (2004) *J. Biol. Chem.* **279**, 48491–48494
- Caldwell, R. A., Boucher, R. C., and Stutts, M. J. (2004) *Am. J. Physiol. Cell Physiol.* **286**, 190–194
- Caldwell, R. A., Boucher, R. C., and Stutts, M. J. (2005) *Am. J. Physiol. Lung Cell. Mol. Physiol.* **288**, 813–819